Quantum-defect theory of resonant charge exchange

Ming Li* and Bo Gao†

Department of Physics and Astronomy, University of Toledo, Mailstop 111, Toledo, Ohio 43606, USA and
State Key Laboratory of Low-Dimensional Quantum Physics, Department of Physics, Tsinghua University, Beijing 100084, China

(Received 22 May 2012; published 24 July 2012)

We apply the quantum-defect theory for $-1/R^4$ potential to study the resonant charge exchange process. We show that by taking advantage of the partial-wave-insensitive nature of the formulation, resonant charge exchange of the type of $^1S + {}^2S$ can be accurately described over a wide range of energies using only three parameters, such as the *gerade* and the *ungerade* s-wave scattering lengths, and the atomic polarizability, even at energies where many partial waves contribute to the cross sections. The parameters can be determined experimentally, without having to rely on accurate potential-energy surfaces, of which few exist for ion-atom systems. The theory further relates ultracold interactions to interactions at much higher temperatures.

DOI: 10.1103/PhysRevA.86.012707 PACS number(s): 34.10.+x, 34.70.+e, 34.50.Cx

I. INTRODUCTION

With the recent emergence of cold-ion experiments, either with trapped ions [1–5] or in the context of cold plasmas [6], there is a growing interest in ion-atom interactions at cold temperatures [7–9], including, in particular, the resonant charge exchange process (see, e.g., Refs. [10–12]), such as

$$\mathrm{Na}^+ + \mathrm{Na} \longrightarrow \mathrm{Na} + \mathrm{Na}^+.$$

Despite being one of the simplest reactive processes that has been a subject of study for a long time [13], *quantitative* understanding of resonant charge exchange remains difficult, especially at cold temperatures. This difficulty stems from its sensitive dependence on the potential-energy surfaces (PES), a common difficulty shared by all heavy particle interactions at cold temperatures (see, e.g., [14]), including not only ion-atom interaction, but also atom-atom interactions [15], and chemical reactions whenever the Langevin assumption breaks down [16,17].

In the case of atom-atom interaction, this difficulty has only been overcome by incorporating a substantial amount of spectroscopic data, especially data close to the dissociation limit, to fine tune the PES (see, e.g., Refs. [18,19]). Without such fine tuning, no *ab initio* PES for alkali-metal systems has been sufficiently accurate to predict the scattering length and other scattering characteristics around the threshold. The availability of such data, however, is limited mostly to alkali-metal atoms and a few other species that can be cooled. For ion-atom systems, with a few exceptions that came close [20], no such data are yet available, though recent efforts on the trapping and cooling of molecular ions (see, e.g., Refs. [21–24]) show considerable future promise. This status on the ion-atom PES is such that at the moment, with the possible exception of $\mathrm{H}^+ + \mathrm{H}$ and its isotopic variations [11,25,26], no other predictions for cold or ultracold ion-atom processes, including resonant charge exchange, can yet be trusted before experimental verification.

We present here a quantum-defect theory (QDT), not only as a general approach to ion-atom interactions, but also as one specific method of dealing with this difficulty of sensitive dependence on PES. It is an initial application of the QDT for $-1/R^4$ potential [8,27,28], as formulated in Ref. [8], to the resonant charge exchange process. We show that by taking advantage of the partial-wave-insensitive nature of the QDT formulation [8,29,30], resonant charge exchange of the type of $^1S + {}^2S$, applicable to group IA (alkali metal), group IIA (alkaline-earth metal), and helium atoms in their ground states, can be accurately described over a wide range of energies using only three parameters, such as the *gerade* and the *ungerade* s-wave scattering lengths, and the atomic polarizability, even at energies where many partial waves contribute to the cross sections. The parameters can be determined experimentally, without having to rely on accurate PESs. The theory further relates ultracold ion-atom interactions to interactions at much higher temperatures. It is the beginning of a much broader program aimed at connecting ultracold interactions and reactions of all types to their behaviors at much higher energies and/or temperatures that are more relevant to astrophysics and everyday chemistry.

For simplicity, and for purposes of making connections with existing formulations and setting benchmarks for further theoretical developments, we adopt here the so-called elastic approximation (see, e.g., Refs. [10,12]) which ignores the hyperfine and isotope effects. Going beyond this approximation will require a multichannel quantum-defect theory (MQDT) formulation of near-resonant charge exchange, along the lines of Refs. [14,31] and similar in spirit to recent works of Idziaszek and co-workers [7,9]. Such a theory will be better understood after the conceptual and numerical developments of this work, which relies only on the single-channel QDT [8]. The multichannel formulation will be presented in a future publication.

The paper is organized as follows. In Sec. II A, we outline the application of QDT to the resonant charge exchange of the type of $^1S + {}^2S$. Section II B discusses two equivalent three-parameter descriptions derived from the QDT formulation. In Sec. III, the three-parameter QDT description is thoroughly tested for the case of resonant charge exchange of ^{23}Na, both through comparison with previous results of Côté and Dalgarno [10], and by comparing our own numerical results with the corresponding QDT parametrization results. We conclude in Sec. IV with further discussions on the implications of our results in the more general context of ion-atom interactions.

*ming.li3@rockets.utoledo.edu
†bo.gao@utoledo.edu

II. QDT OF RESONANT CHARGE EXCHANGE

A. General considerations for $^1S + {}^2S$ type of systems

Consider the system of an atom and its ion, one in a ^1S state, one in a ^2S state. This type covers resonant charge exchange of both group IA (alkali metal), group IIA (alkaline-earth metal), and helium atoms in their ground states. Such a system correlates to two Born-Oppenheimer molecular states, characterized by $^2\Sigma_{g,u}{}^+$. The other, energetically higher, electronic states can be ignored for collision energies much smaller than the first electronic excitation energy [13]. In the case of exact resonance or in the elastic approximation which ignores hyperfine structures and/or the isotope shifts, the two coupled radial Schrödinger equations in the atomic basis become decoupled in the molecular basis, reducing the understanding of resonant charge exchange to two single-channel equations for the *gerade*, g, and the *ungerade*, u, states, respectively [10,12,13],

$$\left[-\frac{\hbar^2}{2\mu}\frac{d^2}{dR^2}+\frac{\hbar^2 l(l+1)}{2\mu R^2}+V_{g,u}(R)-\epsilon\right]u_{\epsilon l}^{g,u}(R)=0. \quad (1)$$

Here μ is the reduced mass, ϵ is the energy in the center-of-mass frame, $V_{g,u}(R)$ represent the two potential-energy curves for the *gerade* and the *ungerade* states, and $u_{\epsilon l}^{g,u}(R)$ are the corresponding radial wave functions for the lth partial wave.

In terms of the two phase shifts, $\delta_l^{g,u}$, for the *gerade* and *ungerade* states in partial wave l, as determined from the solutions of Eq. (1), the total charge exchange cross section $\sigma_{\rm ex}$ can be written as [10,12,13]

$$\sigma_{\rm ex}(\epsilon)=\frac{\pi}{k^2}\sum_{l=0}^{\infty}(2l+1)\sin^2\left(\delta_l^g-\delta_l^u\right). \quad (2)$$

It contains the physical concept that resonant charge exchange is due to the phase difference between the *gerade* and the *ungerade* molecular states. For elastic and total cross sections, it is convenient to first define two single-channel "molecular" cross sections,

$$\sigma^{g,u}=\frac{4\pi}{k^2}\sum_{l=0}^{\infty}(2l+1)\sin^2\left(\delta_l^{g,u}\right), \quad (3)$$

in terms of which the total cross section is given by $\sigma_{\rm tot}=(\sigma^g+\sigma^u)/2$, and the elastic cross section is given by $\sigma_{\rm el}=\sigma_{\rm tot}-\sigma_{\rm ex}$ [10,12,13].

For a $^1S + {}^2S$ type of system with either a ^1S or a ^2S atom in its ground state, the potentials $V_{g,u}(r)$ in Eq. (1) have the same leading term $-C_4/R^4$ at long range, where $C_4>0$ is given in atomic units by $C_4=\alpha_1/2$ with α_1 being the static dipole polarizability of the atom. Application of the single channel QDT for $-1/R^4$ type of potential [8] gives an efficient characterization of the phase shifts $\delta_l^{g,u}$, leading to an efficient characterization of the resonant charge exchange process.

Specifically, for a potential with a long-range behavior of $V\sim -C_n/R^n$, the tangent of the phase shift is given in QDT by [30]

$$\tan\delta_l=\left(Z_{gc}^{c(n)}K^c-Z_{fc}^{c(n)}\right)\left(Z_{fs}^{c(n)}-Z_{gs}^{c(n)}K^c\right)^{-1}. \quad (4)$$

Here $K^c(\epsilon,l)$ is a dimensionless short-range K^c matrix [30]. $Z_{xy}^{c(n)}(\epsilon_s,l)$ are universal QDT functions for the $-1/R^n$ type of potential. They are functions of the angular momentum l and a scaled energy $\epsilon_s=\epsilon/s_E$, where $s_E=(\hbar^2/2\mu)(1/\beta_n)^2$ is the energy scale and $\beta_n=(2\mu C_n/\hbar^2)^{1/(n-2)}$ is the length scale for the $-C_n/R^n$ potential. Explicit expressions for $Z_{xy}^{c(n=4)}$, applicable to the polarization potential, are given in the Appendix. As explained in Ref. [30], Eq. (4) includes not only the effect of long-range phase shift, but also effects of quantum reflection and tunneling, which are the key differences between long-range potentials with $n>2$ and those with $n<2$.

All cross sections for resonant charge exchange can be written explicitly in terms of $\tan\delta_l^g$ and $\tan\delta_l^u$ for the *gerade* and the *ungerade* states,

$$\sigma_{\rm ex}(\epsilon)=\frac{\pi}{k^2}\sum_{l=0}^{\infty}(2l+1)\frac{\left(\tan\delta_l^g-\tan\delta_l^u\right)^2}{\left(1+\tan^2\delta_l^g\right)\left(1+\tan^2\delta_l^u\right)} \quad (5)$$

and

$$\sigma^{g,u}=\frac{4\pi}{k^2}\sum_{l=0}^{\infty}(2l+1)\frac{\tan^2\left(\delta_l^{g,u}\right)}{1+\tan^2\left(\delta_l^{g,u}\right)}. \quad (6)$$

For sufficiently large l and away from a shape resonance, $\tan\delta_l$ is independent of the short-range parameter and is given, for both g and u states, by the Born approximation (see, e.g., Ref. [32]),

$$\tan\delta_l\sim\frac{\pi}{(2l+3)(2l+1)(2l-1)}\epsilon_s. \quad (7)$$

This $1/l^3$ type of behavior for large l ensures convergence in summations over l in all total cross-section calculations.

The application of QDT allows the description of resonant charge exchange in terms of the C_4 coefficient, equivalently the atomic polarizability α_1, and two short-range K matrices, $K_g^c(\epsilon,l)$ for the *gerade* state and $K_u^c(\epsilon,l)$ for the *ungerade* state. Such a description is exact if the energy and the partial wave dependences of the K^cs are fully accounted for. More importantly, QDT allows for efficient parametrizations of resonant charge exchange by taking advantage of the fact that the short-range K^c matrices depend not only weakly on energy, but also weakly on the partial wave l for both atom-atom and ion-atom interactions [8,29,30]. Through an example of $Na^+ + Na$, we show that even the simplest parametrization, corresponding to ignoring the ϵ and l dependences of the K^cs completely, provides an accurate description of resonant charge exchange over a wide range of energies, including energies at which tens of partial waves contribute.

B. Three-parameter QDT descriptions

A three-parameter parametrization of resonant charge exchange for a $^1S + {}^2S$ system results from ignoring both the energy and the partial wave dependences of $K_g^c(\epsilon,l)$ and $K_u^c(\epsilon,l)$. Specifically, it corresponds to the approximation of $K_g^c(\epsilon,l)\approx K_g^c(\epsilon=0,l=0)$ and $K_u^c(\epsilon,l)\approx K_u^c(\epsilon=0,l=0)$. Using K_g^c and K_u^c as the shorthand notation for the resulting constant K^cs, we have one of the three-parameter parametrizations for resonant charge exchange, with two short-range parameters K_g^c and K_u^c, characterizing the short-range ion-atom interaction, and one long-range parameter C_4 or the atomic polarizability α_1, characterizing the strength of the long-range interaction.

A mathematically equivalent three-parameter parametrization is in terms of two s wave scattering lengths, $a_{gl=0}$ and $a_{ul=0}$, for the *gerade* and the *ungerade* state, respectively, and the atomic polarizability α_1. This is derived from the first parametrization by noting that the $K^c(\epsilon = 0, l = 0)$, for both g and u states, are related rigorously to the corresponding s-wave scattering lengths by [33,34]

$$a_{l=0}/\beta_n = \left(b^{2b}\frac{\Gamma(1-b)}{\Gamma(1+b)}\right)\frac{K^c(0,0)+\tan(\pi b/2)}{K^c(0,0)-\tan(\pi b/2)}, \quad (8)$$

where $b = 1/(n-2)$. It reduces to, for $n = 4$,

$$a_{l=0}/\beta_4 = \frac{K^c(0,0)+1}{K^c(0,0)-1}. \quad (9)$$

We note that in the context of the effective range theory [35–38], the three parameters, $a_{gl=0}$, $a_{ul=0}$, and α_1, can only be expected to describe ion-atom interaction in the ultracold regime as characterized by $\epsilon \ll s_E$, in which only the s wave makes a significant contribution. The QDT for ion-atom interaction asserts that the very same set of parameters can in fact describe ion-atom interaction over a much wider range of energies, of the order of $10^5 s_E$, as tested in the next section for ^{23}Na and expected to be qualitatively the same for all alkali-metal atoms.

The two equivalent parametrizations are complementary in terms of the physical understanding that they provide. The parametrization using K^c_g, K^c_u, and α_1 gives a more direct insight as to why it works over a wide range of energies. It is because K^c_g and K^c_u are short-range parameters that are both insensitive to ϵ and l [8,29,30]. The parametrization using $a_{gl=0}$, $a_{ul=0}$, and α_1 enforces the concept that the understanding of ultracold interaction immediately provides understanding of interactions over a much wider range of energies through QDT. This is because embedded in the knowledge of the scattering lengths, $a_{gl=0}$ and $a_{ul=0}$, is the knowledge of the K^c_g and K^c_u parameters, through Eq. (8).

III. EXAMPLE OF $Na^+ + Na$

Low-energy $Na^+ + Na$ charge exchange for ^{23}Na has been studied in detail by Côté and Dalgarno in Ref. [10], within the elastic approximation. It serves as a prototypical system to test the QDT formulation for resonant charge exchange, in particular the range of validity of the three-parameter description.

In Sec. III A, we make a preliminary evaluation of the QDT description by showing, visually, that a three-parameter QDT parametrization, using parameters as given in Ref. [10], reproduces the cross sections of Ref. [10], including all the resonance structures, without any knowledge of the short-range potential. A more detailed comparison is not possible since Ref. [10] made use of unpublished potential-energy results by Magnier *et al*. that are unavailable to us.

For a more detailed comparison between fully quantum numerical calculations and three-parameter QDT results, we construct in Sec. III B the $^2\Sigma_g{}^+$ and $^2\Sigma_u{}^+$ potential curves for $^{23}Na_2{}^+$ using the same procedure as prescribed in Ref. [10], except by using the later published results of Magnier *et al*. [39] in an intermediate region. These potentials are meant to be as close to those of Ref. [10] as possible. Fully quantum numerical calculations of cross sections are carried out with these potentials and compared to the results of corresponding three-parameter QDT descriptions, and also to the earlier results of Côté and Dalgarno [10].

In both sets of calculations, we take the sodium static dipole polarizability to be $\alpha_1 = 162.7$ a.u. [40], the same as that adopted by Côté and Dalgarno [10]. The corresponding length scale for $^{23}Na_2{}^+$ is $\beta_4 = (2\mu C_4/\hbar^2)^{1/2} = 1846 a_0$, where a_0 is the Bohr radius, and the corresponding energy scale is $s_E/k_B = 2.21\ \mu$K or $s_E/h = 46.05$ kHz.

A. Comparison of QDT results with previous results

Numerical results of the "molecular" cross sections for $^2\Sigma_g{}^+$ and $^2\Sigma_u{}^+$ states, as defined by Eq. (3), are given for energies ranging 10^{-16}–1 a.u. in Ref. [10]. The reference also gives the zero energy s-wave scattering lengths for $^2\Sigma_g{}^+$ and $^2\Sigma_u{}^+$ states,

$$a_{gl=0} = 763.3 a_0, \quad (10a)$$

$$a_{ul=0} = 7721.4 a_0. \quad (10b)$$

These s-wave scattering lengths, plus the Na polarizability of $\alpha_1 = 162.7$ a.u. [40], give us all the parameters required for a three-parameter QDT description of resonant charge exchange, from which all relevant cross sections can be calculated, without detailed knowledge of the potentials.

Specifically, from the s-wave scattering lengths of Eq. (10), we first calculate, using Eq. (9), the short-range K^c parameters K^c_g and K^c_u, and obtain

$$K^c_g = -2.4095, \quad (11a)$$

$$K^c_u = 1.6286. \quad (11b)$$

In the three-parameter QDT description, they are taken as constants applicable at all energies and for all partial waves. These parameters, together with the QDT equation for the phase shift, Eq. (4), give us all phase shifts and all cross sections. The results for the total and partial "molecular" cross sections for the $^2\Sigma_g{}^+$ and the $^2\Sigma_u{}^+$ states are illustrated in

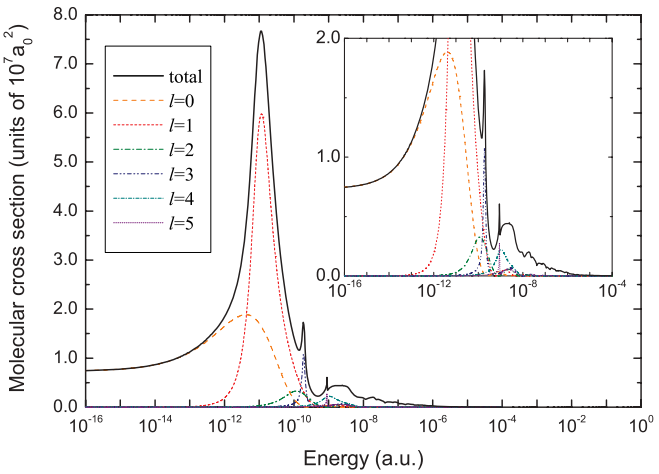

FIG. 1. (Color online) The total and the partial "molecular" cross sections for the $^2\Sigma_g{}^+$ state of $^{23}Na_2{}^+$ from a three-parameter QDT calculation using $a_{gl=0} = 763.3 a_0$, $a_{ul=0} = 7721.4 a_0$, and $\alpha_1 = 162.7$ a.u., all from Ref. [10]. It is to be compared with Fig. 2 of Ref. [10]. The total cross section is obtained by summing over all partial waves until convergence.

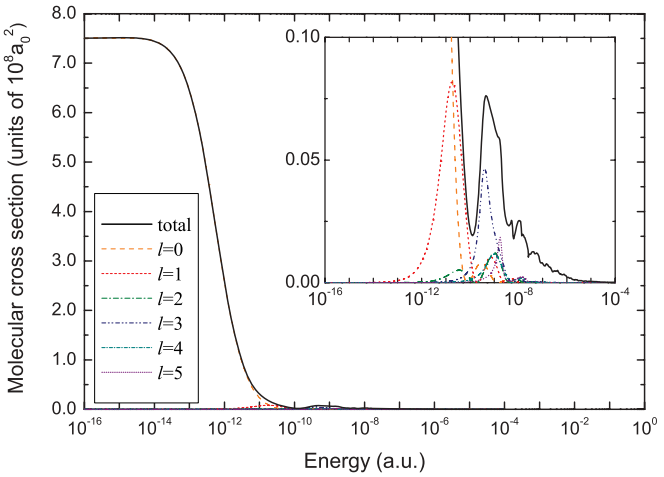

FIG. 2. (Color online) The same as Fig. 1 except that it is for the $^2\Sigma_u{}^+$ state of $^{23}Na_2{}^+$. This figure is to be compared with Fig. 3 of Ref. [10].

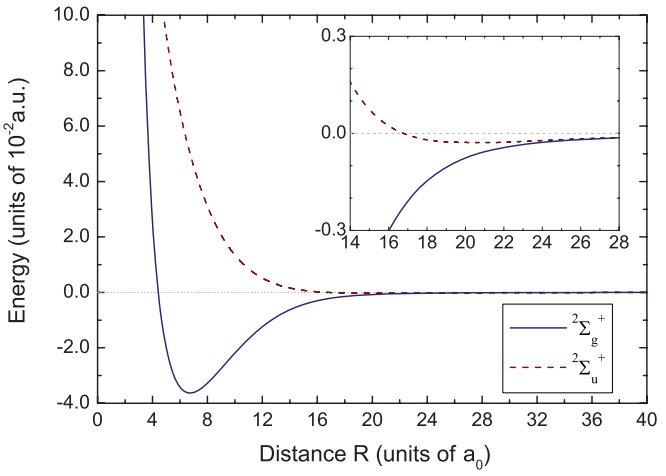

FIG. 3. (Color online) Potential-energy curves for $^2\Sigma_g{}^+$ and $^2\Sigma_u{}^+$ states of $Na_2{}^+$ adopted in our numerical calculations. It can be compared to Fig. 1 of Ref. [10].

Figs. 1 and 2, respectively. They are visually nearly identical to the corresponding results shown in Figs. 2 and 3 of Ref. [10]. All detailed features of the cross sections that are visible in the figures are found to be at the right places judged by visual examination. The results show, at least tentatively, that the three-parameter QDT description can provide an accurate account of resonant charge exchange over a wide range of energies, including all the complex structures which in this case are shape resonances from a wide range of partial waves.

B. More detailed comparison of QDT and numerical results

For a more detailed comparison between fully quantum numerical results and three-parameter QDT calculations, we construct here a version of the $^2\Sigma_g{}^+$ and $^2\Sigma_u{}^+$ potential curves for $Na_2{}^+$. Numerical results are calculated using these potentials and compared to the QDT results corresponding to the same potentials.

1. Potential-energy curves adopted

For both $^2\Sigma_g{}^+$ and $^2\Sigma_u{}^+$ states of $Na_2{}^+$, we use the *ab initio* data of Magnier *et al.* [39] ranging $5.0a_0$–$20.0a_0$. Outside of this region, the potentials are extended using the same procedure as prescribed in Ref. [10], in the hope of getting potentials as close to those of Ref. [10] as possible. Specifically, for distance larger than $22.0a_0$, we extended the potential by the asymptotic form of [10]

$$V_{g,u}(R) = V_{\rm disp}(R) \mp V_{\rm exch}(R), \tag{12}$$

with $\mp$ for $^2\Sigma_g{}^+$ and $^2\Sigma_u{}^+$, respectively. The dispersion term and exchange term are given by [10]

$$V_{\rm disp}(R) = -\frac{C_4}{R^4} - \frac{C_6}{R^6} - \frac{C_8}{R^8}, \tag{13}$$

$$V_{\rm exch}(R) = \frac{1}{2} A R^a e^{-bR} \left(1 + \frac{B}{R}\right). \tag{14}$$

Except for different notations,[1] all coefficients are taken to be the same as in Ref. [10], which, in atomic units, are given by $C_4 = \alpha_1/2 = 81.35$, $C_6 = 936.5$, $C_8 = 27069.5$, $A = 0.111$, $a = 2.254$, $b = 0.615$, and $B = 0.494$. Potential energies between $20.0a_0$ and $22.0a_0$ are interpolated using a cubic spline [41] to make a smooth connection between the *ab initio* data and the long-range behavior. At short distances ($R < 5.0a_0$), we extended the potential with an exponential wall as in Ref. [10],

$$V(R) = W \exp(-wR)\ , \tag{15}$$

with

$$W = V(R)\exp(wR)|_{5.0a_0}, \quad w = -\left.\frac{\partial \ln V(R)}{\partial R}\right|_{5.0a_0}. \tag{16}$$

The resulting $^2\Sigma_g{}^+$ and $^2\Sigma_u{}^+$ potentials for $Na_2{}^+$, thus constructed, are illustrated in Fig. 3. They have the same long-range behavior as those of Ref. [10], and differ only slightly in the short range due to slightly different *ab initio* data adopted.

2. Comparison of QDT and numerical results

For the QDT calculations, we first calculate the parameters K_g^c and K_u^c, more specifically the $K_g^c(\epsilon = 0, l = 0)$ and $K_u^c(\epsilon = 0, l = 0)$ from the potentials. The radial wave function is matched to

$$u_{\epsilon l}(r) = A_{\epsilon l}\left[f^c_{\epsilon_s l}(r_s) - K^c(\epsilon, l) g^c_{\epsilon_s l}(r_s)\right], \tag{17}$$

at progressively larger R until the resulting K^c converges to a constant to a desired accuracy [29,30,33]. Here f^c and g^c are the zero-energy QDT reference functions for the $-1/R^4$ potential [30,34]. We obtain

$$K_g^c = -1.5953, \tag{18a}$$

$$K_u^c = 0.25416. \tag{18b}$$

[1]Our C_4, C_6, and C_8 are denoted as $C_4/2$, $C_6/2$, and $C_8/2$ in Ref. [10]

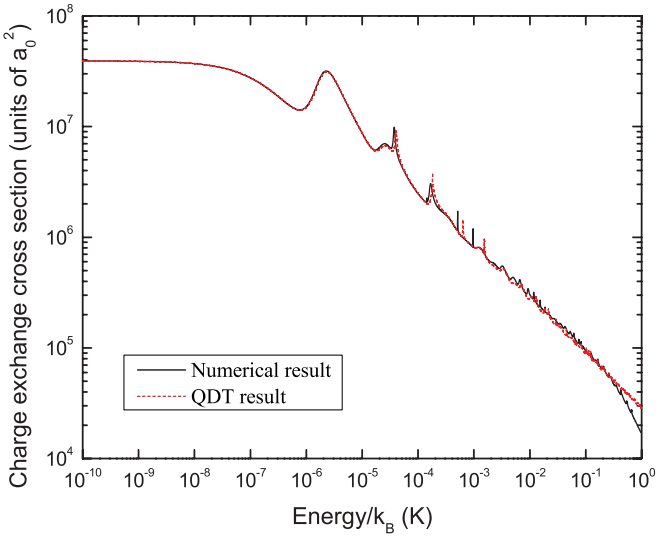

FIG. 4. (Color online) Comparison of the charge exchange cross sections of ^{23}Na obtained from a three-parameter QDT description (dashed line) and from numerical calculations (solid line).

From the K^cs, the s-wave scattering lengths can be obtained by substitution into Eq. (9). We obtain

$$a_{gl=0} = 423.51a_0, \tag{19a}$$

$$a_{ul=0} = -3104.8a_0. \tag{19b}$$

We note in passing that this method of calculating the scattering length converges at much smaller R and provides a more accurate result than by matching to the free-particle solutions or by matching the phase shift to the effective range expansion [10,38], especially for cases with $a_{l=0} \gg \beta_4$.

Our numerical calculations of the phase shifts and cross sections are carried out using a log-derivative method [42,43]. Figure 4 shows the comparison of the charge exchange cross sections obtained from numerical calculations and from the three-parameter QDT description. Figure 5 shows a similar

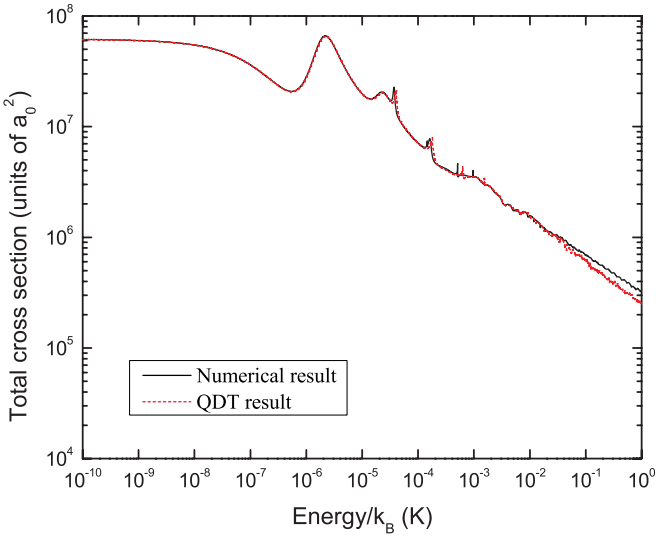

FIG. 5. (Color online) Comparison of the total cross sections of $^{23}Na^+ + {}^{23}$Na obtained from a three-parameter QDT description (dashed line) and from numerical calculations (solid line).

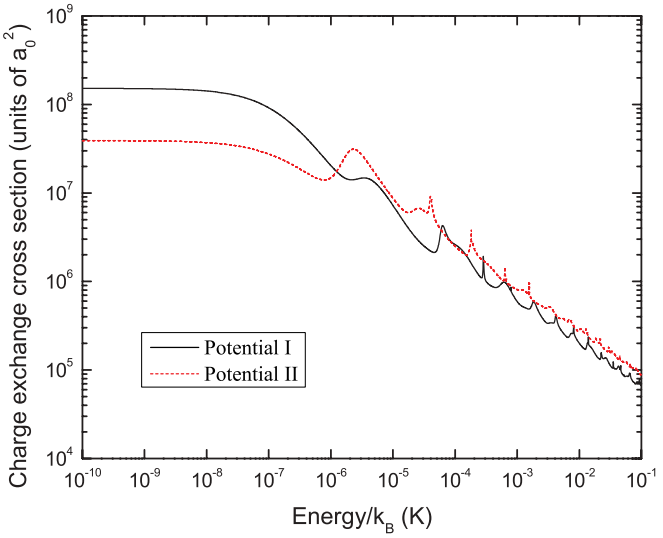

FIG. 6. (Color online) Comparison of charge exchange cross sections of ^{23}Na for two potentials both using three-parameter QDT description. Solid line: results for the potential of Ref. [10]. Dashed line: results for our potential.

comparison of the total cross sections. They both show that the QDT description and the numerical results are in excellent agreement for energies below 0.2 mK. For energy between 0.2 mK and 0.1 K, the QDT prediction still works well with the only discernible differences being due to shape resonances in high partial waves. A better QDT description of such resonances is possible, but is beyond the scope of this work that focuses on the simplest parametrization. Overall, the QDT prediction is satisfactory below 0.1 K, or about $10^5 s_E$. For energy higher than 0.1 K, the discrepancy between the two results grows larger.

The considerable differences between the scattering lengths for our potentials, as given by Eq. (19), and for the potentials of Ref. [10], as given in Eq. (10), are illustrations of the sensitive dependence of cold or ultracold ion-atom interactions on the short-range potential. The two sets of potentials have the same long-range behaviors as characterized by Eqs. (12)–(14), and differ only slightly in the short range, to a degree that is visually indistinguishable on the scale of Fig. 3. Figures 6 and 7, which compare QDT results for the two sets of potentials, give a more complete picture of this dependence. They show that the interactions in the ultracold regime are the most sensitive to the short-range potential. Beyond the ultracold regime of $\epsilon \sim< s_E$, the shape resonance positions remain sensitive to the potential and the QDT parameters over a considerable wider range of energies, of the order of 1 mK or about $1000 s_E$. While the sensitive dependence of ion-atom interaction on the potential gradually diminishes at higher energies for the total cross section, it remains to a considerable degree for the charge exchange cross section.

Fortunately, the sensitive dependence of ion-atom interaction on the PESs is fully encapsulated in a few (two) QDT parameters, as shown in Figs. 4 and 5. Instead of from the PESs, this small number of parameters can be determined from a few experimental data points, such as two resonance positions for $Na^+ + Na$, or two binding energy

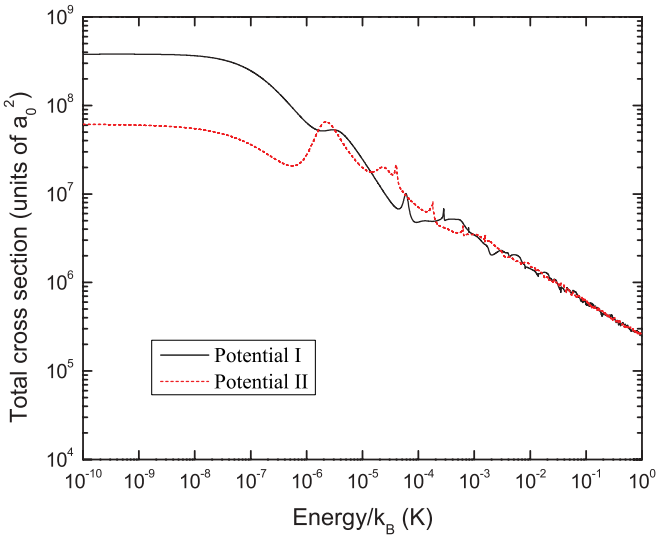

FIG. 7. (Color online) Comparison of total cross sections of $^{23}Na^+ + {}^{23}Na$ obtained from three-parameter QDT descriptions using parameters corresponding to the potential of Ref. [10] (solid line) and using parameters corresponding to our potential (dashed line).

measurements of vibrationally highly excited Na_2^+. Such a determination, in a similar manner as illustrated earlier for atom-atom interaction [29,44], is further facilitated by the concept of universal spectrum including the concept of universal resonance spectrum introduced in Ref. [8] for the $-1/R^4$ potential. We look forward to the availability of experimental data to demonstrate such applications for ion-atom systems.

IV. DISCUSSIONS AND CONCLUSIONS

In conclusion, we have shown that resonant charge exchange of the type of $^1S + {}^2S$ can be accurately described over a wide range of energies using only three parameters, which can either be two short-range K^c matrices, K_g^c and K_u^c, and the atomic polarizability α_1, or two s-wave scattering lengths, $a_{gl=0}$ and $a_{ul=0}$, and α_1. Since the polarizability is well known for most atoms, this is effectively a two-parameter description. Everything else is described by analytic QDT functions for the $-1/R^4$ polarization potential (see Ref. [8] and the Appendix). In the case of ^{23}Na, excellent agreement between the QDT parametrization and numerical results is found from 0 K all the way through 0.1 K, including all resonances within this range. To put this energy range into perspective, we note again that $\epsilon/k_B = 0.1$ K corresponds roughly to $\epsilon_s = \epsilon/s_E \sim 10^5$. At this energy, one can estimate that there are at least $\sqrt{2}\epsilon_s^{1/4} \sim 25$ partial waves contributing to the cross sections. Such a simple parametrization over such a wide range of energies is made possible in QDT not only by the energy insensitivity of the short-range parameters, K_g^c and K_u^c, but also by their partial-wave insensitivity [8,29,30]. The energy insensitivity is ensured here by the large length scale separation as is typical for ion-atom interactions. More quantitatively, it is reflected in $\beta_6/\beta_4 \approx 6.56 \times 10^{-3}$ for Na, where $\beta_6 = (2\mu C_6/\hbar^2)^{1/4}$ is the length scale associated with the $-C_6/R^6$ term of the potential in Eq. (13). This value gives an order-of-magnitude measure of the length scale separation that is representative of all alkali-metal atoms. The partial-wave insensitivity is ensured by the combination of length scale separation and the smallness of the electron-to-nucleus mass ratio [29,34].

The example of ^{23}Na has also served to illustrate the sensitive dependence of cold or ultracold ion-atom interactions on the PESs. While one can always construct the potentials for ion-atom systems, their accuracies are generally far from sufficient in predicting cold collisions, and the related vibrationally highly excited molecular-ion spectrum [8]. The QDT deals with this difficulty by encapsulating this sensitive dependence into a few short-range parameters that can be determined experimentally. The simplicity of the resulting description has the following implications. (a) Since there are only a few parameters, they can be determined from very few experimental data points. (b) Since the parametrization works over a wide range of energies, it allows the determination of the parameters from measurements of structures (either resonance or binding energy) away from the threshold, where they are much further separated [8] and can be resolved with much less stringent requirement on either the energy resolution or the temperature [20]. This can be an important consideration for ion-atom interactions, where going below mK has been proven to be difficult experimentally. (c) Such a parametrization offers a systematic understanding of a class of systems. For example, the parametrization for $Na^+ + Na$ works the same for all resonant charge exchange processes of the type of $^1S + {}^2S$. Different systems differ only in scaling as determined by the atomic polarizability α_1, and the two short-range parameters. (d) The parameters that are used to characterize interaction in the absence of any external field also characterize the interaction in the presence of external fields, thus relating field-free interactions to interactions within a field [31,45].

This work represents only the simplest QDT description for resonant charge exchange, with a goal of establishing key qualitative features that form the conceptual foundation for further theoretical development. Future works will include rigorous treatments of the hyperfine and isotopes effects, more accurate treatment of resonances in high partial waves which give rise to only deviations of any significance in Figs. 4 and 5, and further extension of the range of energies to room temperatures and above. A realization of these goals, with a theory of a few parameters, will greatly facilitate the incorporation of accurate ion-atom interaction data into simulations of not only cold plasmas [6], but also plasma systems of interest in astrophysics and everyday chemistry and technology. The extension to room temperatures and above will be carried out through the development of a more accurate "semiclassical" approximation. We point out that the existing semiclassical approximation [10], while helpful qualitatively, is not accurate quantitatively. We are hopeful that the QDT formulation will help us in developing and testing a far more accurate "semiclassical" approximation, thus extending our semianalytical, yet precise, description of ion-atom interactions into room temperatures and above.

ACKNOWLEDGMENTS

We thank L. You, S. Federman, and T. Kvale for helpful discussions. The work at Toledo was supported in part by NSF. The work at Tsinghua was supported in part by the National

Science Foundation of China under Grant No. 11004116, and in part by the research program 2010THZO of the Tsinghua University.

APPENDIX: $Z^{c(n)}$ MATRIX FOR $-1/R^4$ POTENTIAL

The $Z^{c(n)}$ matrix is well defined for any $-1/R^n$ type of potentials with $n > 2$ [30]. For the polarization potential corresponding to $n = 4$, its elements are given by

$$Z^{c(4)}_{fs}(\epsilon_s,l) = \frac{\cos[\pi(\nu-\nu_0)/2]}{2M_{\epsilon_s l}\cos(\pi\nu/2)} \times \left\{1-(-1)^l M^2_{\epsilon_s l}\tan[\pi(\nu-\nu_0)/2]\right\}, \quad \text{(A1)}$$

$$Z^{c(4)}_{fc}(\epsilon_s,l) = \frac{\cos[\pi(\nu-\nu_0)/2]}{2M_{\epsilon_s l}\cos(\pi\nu/2)} \times \left\{\tan[\pi(\nu-\nu_0)/2]-(-1)^l M^2_{\epsilon_s l}\right\}, \quad \text{(A2)}$$

$$Z^{c(4)}_{gs}(\epsilon_s,l) = \frac{\cos[\pi(\nu-\nu_0)/2]}{2M_{\epsilon_s l}\sin(\pi\nu/2)} \times \left\{1+(-1)^l M^2_{\epsilon_s l}\tan[\pi(\nu-\nu_0)/2]\right\}, \quad \text{(A3)}$$

$$Z^{c(4)}_{gc}(\epsilon_s,l) = \frac{\cos[\pi(\nu-\nu_0)/2]}{2M_{\epsilon_s l}\sin(\pi\nu/2)} \times \left\{\tan[\pi(\nu-\nu_0)/2]+(-1)^l M^2_{\epsilon_s l}\right\}. \quad \text{(A4)}$$

Here $\nu_0 = l + 1/2$, ν is the characteristic exponent for the $-1/R^4$ potential (corresponding to the modified Mathieu equation [46–48]), and $M_{\epsilon_s l}$ is one of its QDT functions. Their evaluations have been discussed in Ref. [8]. Together with Eqs. (A1)–(A4) for the $Z^{c(4)}$ matrix, they are all the requirements for the implementation of QDT for resonant charge exchange. The derivation of $Z^{c(4)}$, and other aspects of QDT for $-1/R^4$ potential, will be presented in a separate publication.

[1] A. T. Grier, M. Cetina, F. Oručević, and V. Vuletić, Phys. Rev. Lett. **102**, 223201 (2009).
[2] C. Zipkes, S. Palzer, C. Sias, and M. Köhl, Nature (London) **464**, 388 (2010).
[3] C. Zipkes, S. Palzer, L. Ratschbacher, C. Sias, and M. Köhl, Phys. Rev. Lett. **105**, 133201 (2010).
[4] W. G. Rellergert, S. T. Sullivan, S. Kotochigova, A. Petrov, K. Chen, S. J. Schowalter, and E. R. Hudson, Phys. Rev. Lett. **107**, 243201 (2011).
[5] F. H. J. Hall, M. Aymar, N. Bouloufa-Maafa, O. Dulieu, and S. Willitsch, Phys. Rev. Lett. **107**, 243202 (2011).
[6] T. C. Killian, Science **316**, 705 (2007).
[7] Z. Idziaszek, T. Calarco, P. S. Julienne, and A. Simoni, Phys. Rev. A **79**, 010702(R) (2009).
[8] B. Gao, Phys. Rev. Lett. **104**, 213201 (2010).
[9] Z. Idziaszek, A. Simoni, T. Calarco, and P. S. Julienne, New J. Phys. **13**, 083005 (2011).
[10] R. Côté and A. Dalgarno, Phys. Rev. A **62**, 012709 (2000).
[11] E. Bodo, P. Zhang, and A. Dalgarno, New J. Phys. **10**, 033024 (2008).
[12] P. Zhang, A. Dalgarno, and R. Côté, Phys. Rev. A **80**, 030703(R) (2009).
[13] N. F. Mott and H. S. W. Massey, *The Theory of Atomic Collisions* (Oxford University Press, London, 1965).
[14] B. Gao, Phys. Rev. A **54**, 2022 (1996).
[15] C. Chin, R. Grimm, P. Julienne, and E. Tiesinga, Rev. Mod. Phys. **82**, 1225 (2010).
[16] B. Gao, Phys. Rev. Lett. **105**, 263203 (2010).
[17] B. Gao, Phys. Rev. A **83**, 062712 (2011).
[18] R. Ferber, I. Klincare, O. Nikolayeva, M. Tamanis, H. Knöckel, E. Tiemann, and A. Pashov, Phys. Rev. A **80**, 062501 (2009).
[19] S. Knoop, T. Schuster, R. Scelle, A. Trautmann, J. Appmeier, M. K. Oberthaler, E. Tiesinga, and E. Tiemann, Phys. Rev. A **83**, 042704 (2011).
[20] U. Hechtfischer, C. J. Williams, M. Lange, J. Linkemann, D. Schwalm, R. Wester, A. Wolf, and D. Zajfman, J. Chem. Phys. **117**, 8754 (2002).
[21] E. R. Hudson, Phys. Rev. A **79**, 032716 (2009).
[22] J. H. V. Nguyen, C. R. Viteri, E. G. Hohenstein, C. D. Sherrill, K. R. Brown, and B. C. Odom, New J. Phys. **13**, 063023 (2011).
[23] J. H. V. Nguyen and B. Odom, Phys. Rev. A **83**, 053404 (2011).
[24] S. Willitsch, Int. Rev. Phys. Chem. **31**, 175 (2012).
[25] A. Igarashi and C. D. Lin, Phys. Rev. Lett. **83**, 4041 (1999).
[26] B. D. Esry, H. R. Sadeghpour, E. Wells, and I. Ben-Itzhak, J. Phys. B **33**, 5329 (2000).
[27] S. Watanabe and C. H. Greene, Phys. Rev. A **22**, 158 (1980).
[28] I. I. Fabrikant, J. Phys. B **19**, 1527 (1986).
[29] B. Gao, Phys. Rev. A **64**, 010701(R) (2001).
[30] B. Gao, Phys. Rev. A **78**, 012702 (2008).
[31] B. Gao, E. Tiesinga, C. J. Williams, and P. S. Julienne, Phys. Rev. A **72**, 042719 (2005).
[32] L. D. Landau and E. M. Lifshitz, *Quantum Mechanics* (Pergamon, Oxford, 1977).
[33] B. Gao, J. Phys. B **36**, 2111 (2003).
[34] B. Gao, Eur. Phys. J. D **31**, 283 (2004).
[35] J. Schwinger, Phys. Rev. **72**, 738 (1947).
[36] J. M. Blatt and D. J. Jackson, Phys. Rev. **76**, 18 (1949).
[37] H. A. Bethe, Phys. Rev. **76**, 38 (1949).
[38] T. F. O'Malley, L. Spruch, and L. Rosenberg, J. Math. Phys. **2**, 491 (1961).
[39] S. Magnier and F. Masnou-Seeuws, Mol. Phys. **89**, 711 (1996).
[40] C. R. Ekstrom, J. Schmiedmayer, M. S. Chapman, T. D. Hammond, and D. E. Pritchard, Phys. Rev. A **51**, 3883 (1995).
[41] W. T. V. William, H. Press, Saul A. Teukolsky, and B. P. Flannery, *Numerical Recipes: The Art of Scientific Computing*, 3rd ed. (Cambridge University Press, Cambridge, England, 2007).
[42] B. R. Johnson, J. Comput. Phys. **13**, 445 (1973).

[43] D. E. Manonopoulos, J. Chem. Phys. **85**, 6425 (1986).
[44] B. Gao, Phys. Rev. A **58**, 4222 (1998).
[45] T. M. Hanna, E. Tiesinga, and P. S. Julienne, Phys. Rev. A **79**, 040701 (2009).
[46] M. Abramowitz and I. A. Stegun, eds., *Handbook of Mathematical Functions* (National Bureau of Standards, Washington, D.C., 1964).
[47] N. A. W. Holzwarth, J. Math. Phys. **14**, 191 (1973).
[48] D. B. Khrebtukov, J. Phys. A **26**, 6357 (1993).